

# A thermodynamic database for tellurium-bearing systems relevant to nuclear technology

G. Chattopadhyay <sup>a</sup> and J.M. Juneja <sup>b</sup>

<sup>a</sup> Applied Chemistry Division and <sup>b</sup> Metallurgy Division, Bhabha Atomic Research Centre, Bombay 400085, India

Received 4 December 1992; accepted 22 January 1993

A thermodynamic database for tellurium-bearing condensed phases and gaseous species which are relevant to nuclear technology is presented. It contains phase diagrams of the binary systems, Pd–Te, Rh–Te, Pu–Te, Sm–Te, Cs–Te, Zr–Te, of the ternary systems, Zr–Te–O, Mo–Te–O, Ag–Te–O, U–Te–O, Cs–Te–O, Ba–Te–O as well as thermodynamic data for crystalline and liquid Te, for the solid phases Cs<sub>2</sub>Te, Ag<sub>2</sub>Te, SnTe, BaTe, CeTe, SmTe, RuTe<sub>2</sub>, ZrTe<sub>2</sub>, Fe<sub>0.53</sub>Te<sub>0.47</sub>, Mo<sub>0.43</sub>Te<sub>0.57</sub>, Cr<sub>0.43</sub>Te<sub>0.57</sub>, Ni<sub>0.5</sub>Te<sub>0.4</sub>, Cs<sub>2</sub>TeO<sub>3</sub> and for the gaseous species, Te, Te<sub>2</sub>, TeO, TeO<sub>2</sub>, TeO(OH)<sub>2</sub>, H<sub>2</sub>Te, TeI, TeI<sub>2</sub>, TeI<sub>4</sub>, TeOl<sub>2</sub>, SnTe, Sn<sub>2</sub>Te<sub>2</sub>, SnTe<sub>2</sub>.

## 1. Introduction

The chemical consequence of nuclear fission is the generation of 20 and odd important fission products (f.p.) which play a two-fold role in an operating nuclear reactor. Besides modifying the chemical state of the fuel, they also constitute the major hazard of the fission reactors by virtue of their radioactivity. Thus in the ultimate analysis, it is the internal chemistry of the fuel pin which determines the performance of the fuel, influences its reprocessing chemistry, affects the process of disposal of the waste as well as the release behavior of the radioactive isotopes under normal and accident conditions. The question of the chemical state of the irradiated oxide fuels has been studied extensively in the past twenty five years and by now, is well understood. With the aid of equilibrium approximation and thermodynamic data this empirical knowledge is useful in calculating the release behavior of radioactive isotopes under accident conditions. This would also enable the prediction of chemical states for advanced fuel cycles if systematic thermodynamic databases for relevant systems are available. Tellurium being one of the fission products with moderate yield, attention has been focused, in the present work, on a database for tellurium-containing systems.

It is well known that tellurium can cause corrosion of the cladding materials. It can also interact with the fissile elements and other f.p. within the reactor. This

is evident in table 1, which summarizes the various chemical forms in which tellurium is found in the irradiated oxide fuel assembly. Thus the metal–tellurium systems (M–Te) which are relevant to the nuclear technology fall into three categories: (i) those containing Fe, Cr, Ni, Zr, Nb and Sn which constitute the clad, (ii) those involving major fission products such as Mo, Ru, Cs, Zr, Pd, Nd, Ce, Ba, Rh, La, Pr, Sm, Ag etc. and (iii) those containing fissile elements U and Pu. In addition, the corresponding ternary M–Te–O systems are also important as far as the oxide fuels are concerned.

In this paper, an up-to-date and evaluated phase diagram and thermodynamic data for some of the systems mentioned above are presented with particular reference to the experimental techniques employed in the dissociation pressure measurements to highlight the suitability of a given technique for obtaining the needed data.

## 2. The thermodynamic database

The thermodynamic database needed to make any reliable calculation has to take into account all possible phases and species that might form. The database presented here consists of the following information:

- (1) binary phase diagrams of M–Te systems,
- (2) thermodynamic functions of elemental tellurium,

Table 1  
Chemical state of tellurium in irradiated fuel pins <sup>a</sup>

Chemical State	Location
Dissolved in mixed oxide solubility up to 0.27 wt%	–
Pd–Te mixed phases	Central void, within the fuel, in the gap.
Distinct oxides probably as $\text{Pu}_2\text{O}_7\text{Te}$ precipitates (in $\text{PuO}_2$ grains within the unrestructured fuel zone)	Hot fuel end
$(\text{Ba}, \text{Sr})\text{TeO}_3$ , $\text{Pu}_2\text{O}_7\text{Te}$	Near the blankets
Tellurides of Ba and Mo and in less amounts of Cs	Hot end of the gap and in the attached clad.

<sup>a</sup> See, for example, ref. [111].

- (3) dissociation pressures of metal tellurides,
- (4) ternary systems and gaseous species,
- (5) thermodynamic data.

## 2.1. Binary phase diagrams of M–Te systems

The binary phase diagrams form the most primary data base for the thermodynamic analysis of any heterogeneous equilibrium. Therefore, phase diagrams of M–Te systems containing many of the foregoing elements were compiled [1] and evaluated [2]. The latest versions of phase diagrams where M is Fe, Cr, Ni, Zr, Nb, Mo, La, Ru and Ag are given in ref. [2]. Since new informations have become available on Pd–Te [3] and Rh–Te [4] systems, the re-evaluated phase diagram of Pd–Te and newly determined phase diagram of Rh–Te are presented in figs. 1 and 2. Those of Nb–Te, Ru–Te and Zr–Te are incomplete but it is known that in these systems the phases coexisting with the respective metals are  $\text{Nb}_5\text{Te}_4$ ,  $\text{RuTe}_2$  and  $\text{Zr}_3\text{Te}_5$  [5]. Phase diagrams of Sn–Te [6], Nd–Te [7], Ba–Te [8], Pr–Te [9] are available in the literature [1]. The phase diagram of U–Te given in ref. [10] is accepted in the present work. Incomplete phase diagrams of Pu–Te and Sm–Te constructed from the informations available on the various phases in these systems [10,11] are presented in figs. 3

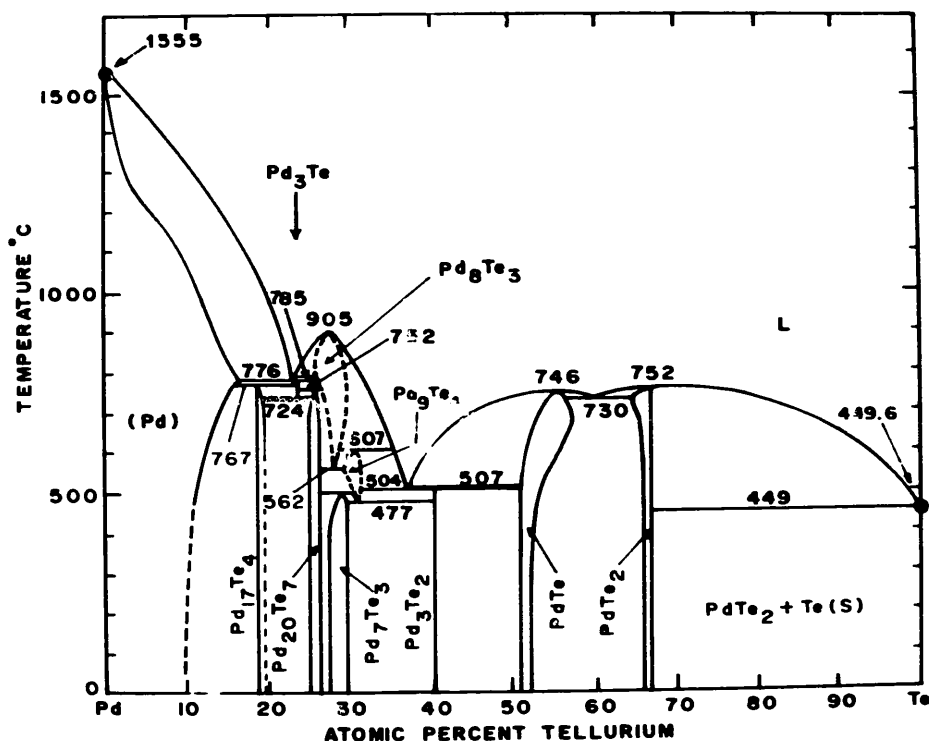


Fig. 1. Phase diagram of the system palladium–tellurium.

and 4, respectively. One complete and another partial phase diagram of Cs–Te system are reported in literature [12,13]. Owing to the complexity of the system, the attainment of equilibrium and the phase relations are uncertain. A tentative phase diagram of Cs–Te constructed from the recent literature data [12–16] is given in fig. 5.

## 2.2. Thermodynamic functions of elemental tellurium

Thermodynamic functions of elemental tellurium are of prime importance in calculating the thermodynamic properties of metal tellurides. These functions for crystalline and liquid tellurium were compiled by

Hultgren et al. [17], Mills [18], Gronvold et al. [19] and Brebrick [20]. The first two were based on heat capacity equations of Kubaschewski and Wittig [21]. Gronvold et al. [19] combined their own heat capacity data [22] with those of Anderson [23], Slansky and Coulter [24] and Leadbetter and Jeapes [25]. Brebrick [20] used heat capacity data of Medzhidov and Rasulov [26] and of Takeda, Okazaki and Tamaki [27]. Thermodynamic functions for the gas phase, in which Te and  $\text{Te}_2$  are by far the most important species, are given for Te(g), based on the electronic term values tabulated by Moore [28] which are principally derived from the experiments of Ruedy [29]. Thermodynamic functions for  $\text{Te}_2(\text{g})$  are given by Stull and Sinke [30], Hultgren et al. [17], Mills

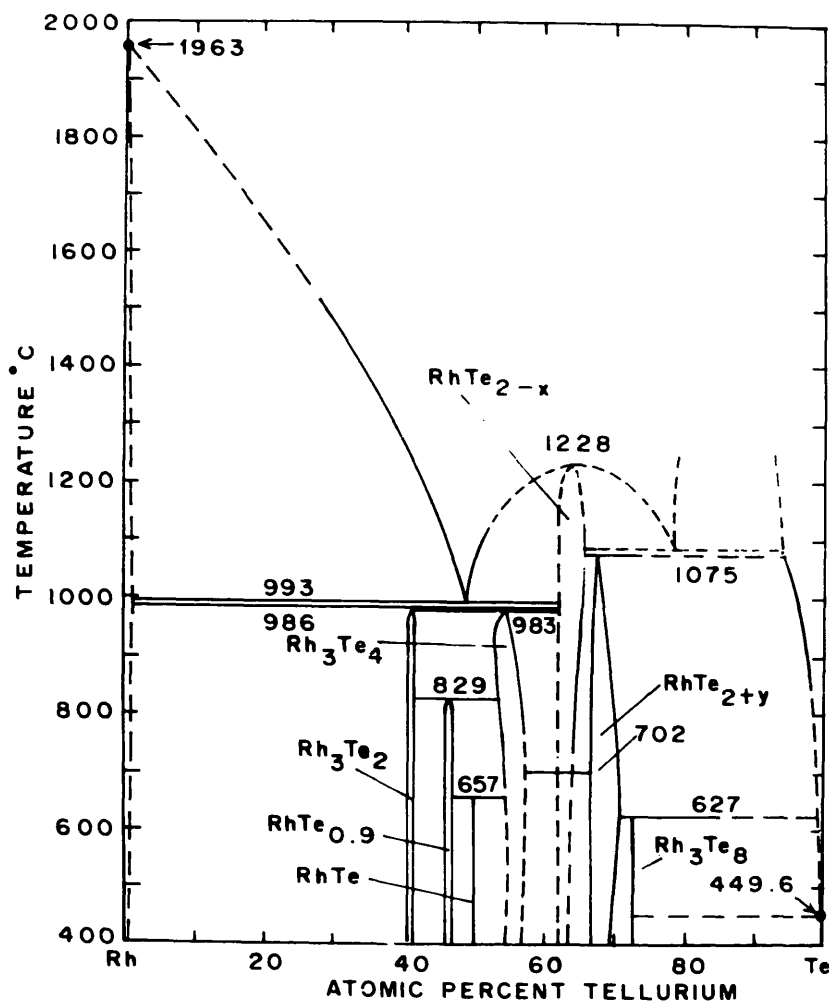


Fig. 2. Phase diagram of the system rhodium–tellurium.

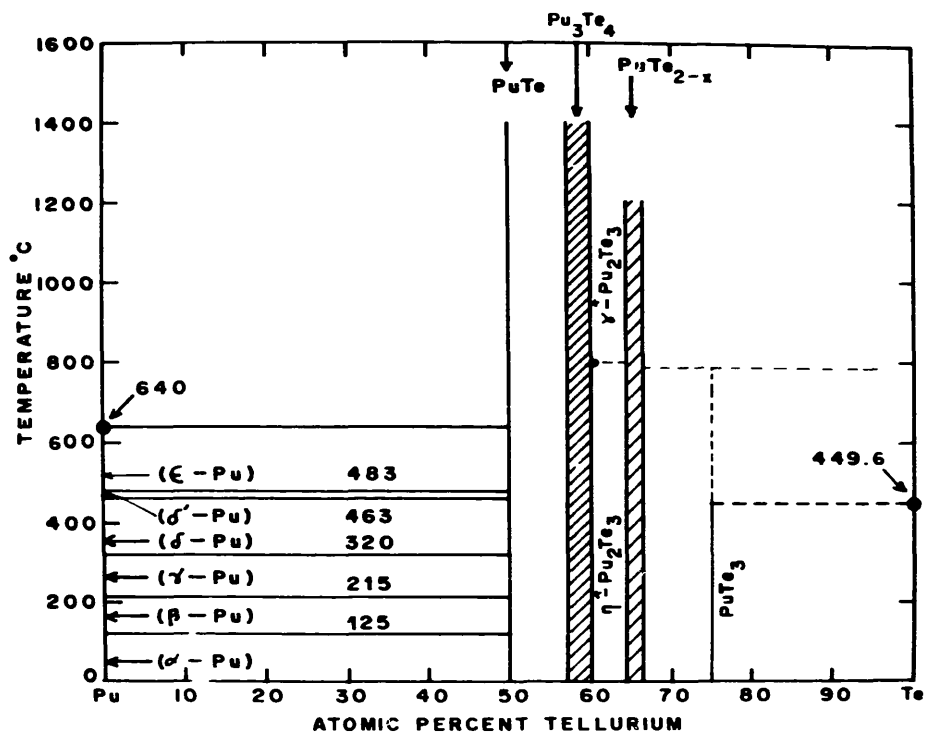


Fig. 3. Phase diagram of the system plutonium-tellurium.

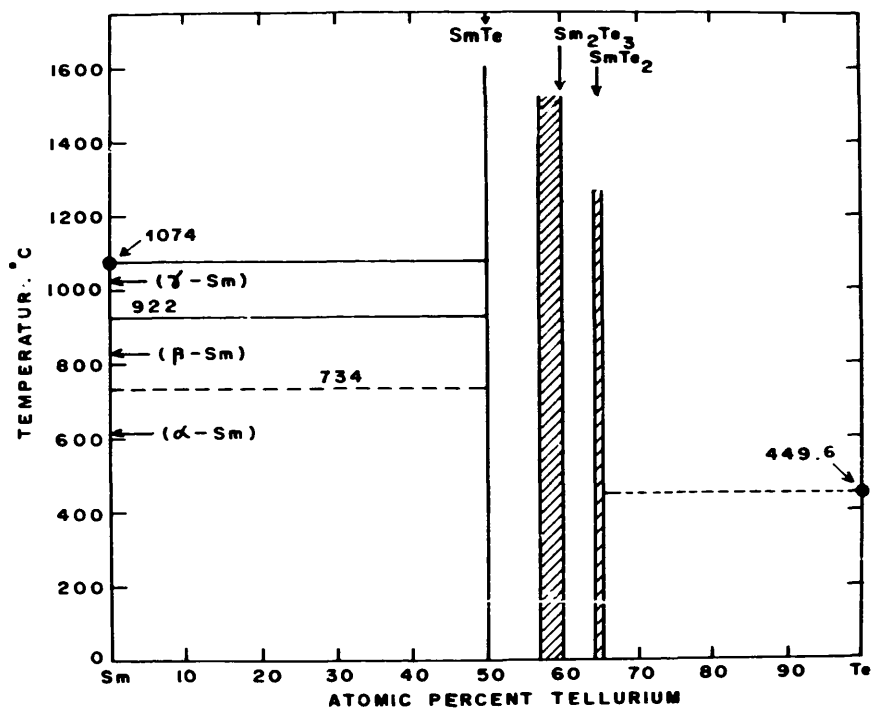


Fig. 4. Phase diagram of the system samarium-tellurium.

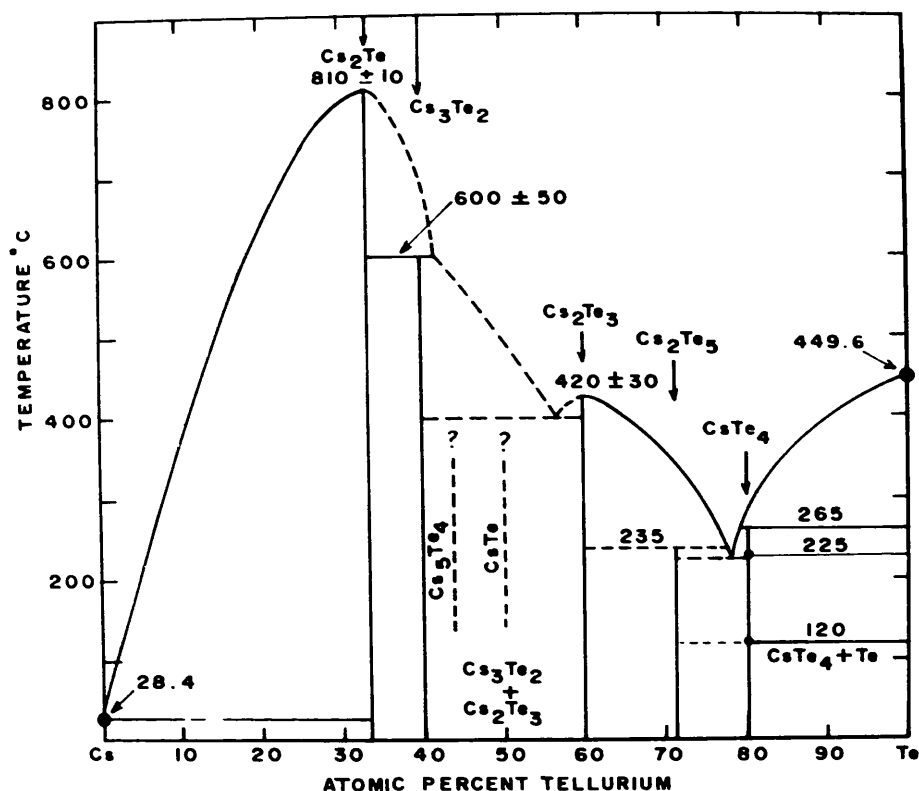


Fig. 5. Phase diagram of the system caesium-tellurium.

[18], Svendsen [31] and Gronvold et al. [19]. The last named authors have improved upon the previous data by taking into account the recent spectroscopic measurements [32–37]. Verges et al. [32] have determined the dissociation energy of  $\text{Te}_2(\text{g})$ . Brebrick [20] also recalculated the thermodynamic functions for  $\text{Te}_2(\text{g})$  from the known spectroscopic functions [38,39]. The values given by Gronvold et al. [19] and Brebrick [20] are in good agreement.

### 2.2.1. Vapor pressure of tellurium

A large number of mass spectrometric investigations [40–49] indicates presence of species  $\text{Te}_n$  where  $n = 1$  to 7 and that besides  $\text{Te}$  and  $\text{Te}_2$ , the other species of any importance are  $\text{Te}_3$  and  $\text{Te}_5$ .

Brebrick [20] has compiled equations for the variation of the total pressure of saturated vapor over  $\text{Te}(\text{c})$  from room temperature to the melting point and over

Table 2

Contribution of  $\text{Te}_2(\text{g})$  to the total pressure of the saturated vapor of  $\text{Te}(\text{c}, \text{l})$

Temperature (K)	$\log p^\circ(\text{total})$ (Pa)	$p^\circ(\text{Te}_2)/p^\circ(\text{total})$		
		(a)	(b)	(c)
600	−0.90	1.0	0.97	0.86
700	1.05	0.97	0.92	0.96
800	2.25	0.958	—	0.90
900	3.10	0.955	—	0.92
1000	3.77	0.947	—	0.93
1100	4.31	0.922	—	0.92
1200	4.75	0.908	—	0.90
1266	5.01	0.899	—	—

(a) Calculated by Gronvold et al. [19] from the mass spectrometric data of Neubert [45], (b) from mass spectrometric data of Viswanathan et al. [49], (c) calculated from  $p^\circ(\text{total})$  and selected thermodynamic functions [19].

Te(l) from the melting point to 1750 K. These are represented by eqs. (1) to (6).

$\log p(\text{Pa})$

$$= -8485.0/T + 13.649 - 6.81577 \times 10^{-4}T \quad (298.15 - 722.65 \text{ K}), \quad (1)$$

$$= -6258.596/T + 10.075006 \quad (722.65 - 800 \text{ K}), \quad (2)$$

$$= -6099.228/T + 9.875657 \quad (800 - 921.6 \text{ K}), \quad (3)$$

$$= -5960.2/T + 9.7284 \quad (921.6 - 1142.5 \text{ K}), \quad (4)$$

$$= -5877.37/T + 9.652377 \quad (1142.5 - 1434.7 \text{ K}), \quad (5)$$

$$= -5719.9/T + 9.5376 \quad (1434.7 - 1750 \text{ K}). \quad (6)$$

Eqs. (1), (2) and (3) were derived by Brebrick [20], eq. (4) was given by Brooks [50] and eqs. (5) and (6) were derived from the data given by refs. [51–53]. Two sets of mass-spectrometric data [45,49] and four sets of total pressure measurements [54–57] are reported over solid Te. The values given by Viswanathan et al. [49] which are larger than the corresponding values of

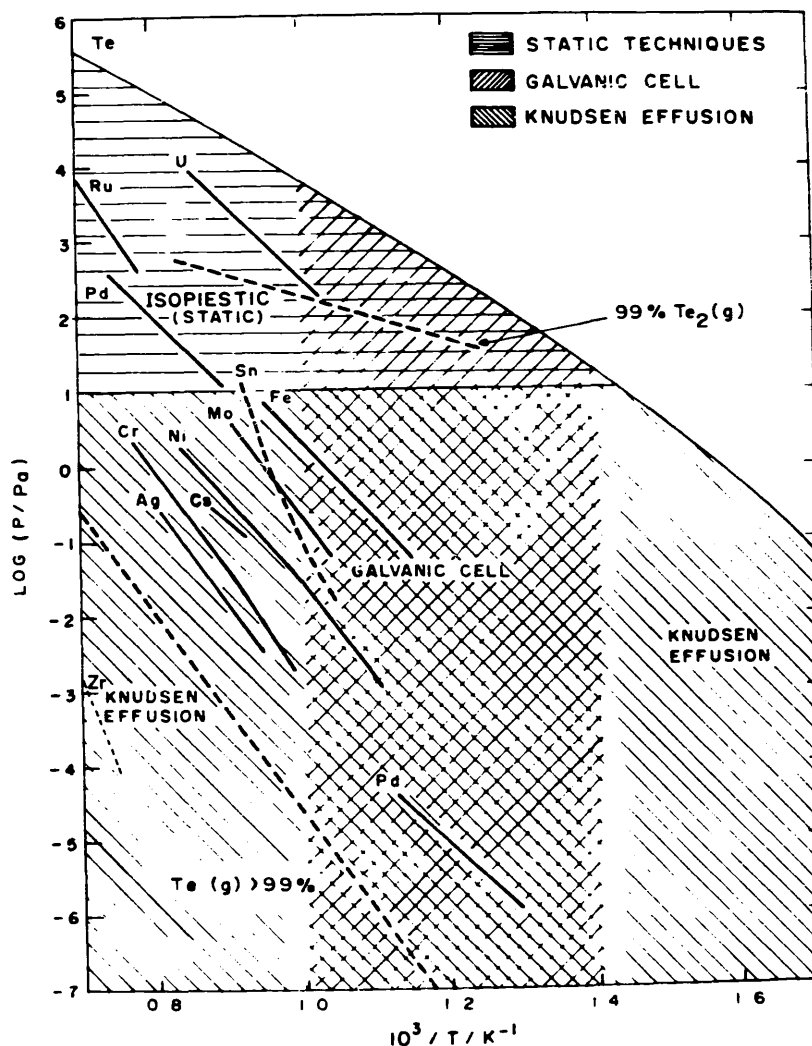


Fig. 6. Dissociation pressure over metal tellurides as a function of reciprocal temperature and the domains of applicability of various experimental techniques.

Neubert [45] by factors of 1.7 and 1.4 at 600 and 700 K, respectively, are in closer agreement with the total pressure measurements [54–67]. The experimental data fall within 20% of the values given by eq. (1). The total pressure  $p^\circ$  (total) in the entire temperature range is plotted against the reciprocal temperature in fig. 6. The curvature of this plot indicates that the composition of the saturated vapor does not change considerably with temperature.

The vapor pressure data yielded the enthalpy of sublimation of  $\text{Te}_2(\text{g})$  at 298 K [17–20]. The value of  $163176 \text{ J mol}^{-1}$  was chosen from the evaluation of ref. [19]. This was combined with various pairs of thermodynamic functions for  $\text{Te}(\text{c}, l)$  and  $\text{Te}_2(\text{g})$  [17–20] to

calculate the values of  $p^\circ(\text{Te}_2)$  and hence, to check the consistency of each pair with the measured vapor pressures. The only pair of free energy functions found to be consistent was that given by Gronvold et al. [19]. To further check the consistency of these values with the experimental data, the ratio  $p^\circ(\text{Te}_2)/p^\circ(\text{total})$  was calculated using the selected thermodynamic functions as well as the mass-spectrometric data [45,49]. The results are given in table 2. The  $p^\circ(\text{Te}_2)/p^\circ(\text{total})$  ratios calculated from the mass-spectrometric data are in fair agreement with the selected thermodynamic values [19], though the mutual agreement between the mass-spectrometric results is poor. Two conclusions can be drawn from table 2: (i) over 90% of the saturated vapor of

Table 3

Partial pressure of Te and  $\text{Te}_2$  over metal tellurides ( $p$  in Pa)

System	Temperature range (K)	$\log p = -A/T + B$		Technique	Ref.
		A	B		
FeTe	870–1020	9232	10.910	KE	[18]
Fe + $\beta$	866–990	9860.5	10.157	Ke–MI	[60]
	885–1048	12227 *	11.03	KE–Ms	[61]
		10759 **	11.12		
Cr + $\text{Cr}_{1-x}\text{Te}$	1100–1260	13935	11.198	KE–MI	[62]
	1185–1285	13135 *	10.46	KE–Ms	[63]
		12974 **	10.35		
Cr + $\text{Cr}_3\text{Te}_4$	1055–1115	20354	17.697	KE–MI	[62]
	1015–1135	14124 *	11.32	KE–Ms	[63]
		14845 **	11.94		
Ni + $\beta_1$	1071–1188	12303	10.399	KE–MI	[64]
	1090–1190	11930 *	9.67	KE–Ms	[65]
		11187 **	9.65		
Ni + $\beta'_1$	1020–1055	11189 *	8.95	KE–Ms	[65]
		10883 **	9.35		
Ni + $\beta_2$	893–993	13350 *	11.11	KE–Ms	[65]
		12563 **	10.95		
Mo + $\text{Mo}_3\text{Te}_4$	960–1100	13381 *	11.82	KE–Ms	[66]
		13287 **	12.663		
		9879	10.56	Bourdon	[67]
Ru + $\text{RuTe}_2$	1276–1423	15020	11.382	Bourdon	[31]
$\text{UTe}_2 + \text{U}_3\text{Te}_5$	973–1173	9577	12.106		[68]
BaTe( <i>l</i> )	1779–1919	20230 *	10.966	KE–MI	[69]
SmTe	1732–1922	20881 *	9.686	KE–MI	[70]
CeTe(c)	1940–2060	24100 *	11.174	KE–Ms	[71]
Ag + $\text{Ag}_2\text{Te}$	1073–1303	19851	17.496	Trans	[72]
	1044–1142	10755 **	8.466	KE–Ms	[73]
	1051–1165	12960 **	9.82	KE–T	[74]
	1130–1232	13800 **	10.529	KE–Ms	[75]
$\text{Pd}_{60}\text{Te}_{40}$	1113–1344	9490	9.61	Isopiestic	[76]
$\text{Pd}_{68}\text{Te}_{32}$	772–889	10470	7.64	cmf	[77]

$\beta$ ,  $\text{Cr}_{1-x}\text{Te}$ ,  $\text{Cr}_3\text{Te}_4$ ,  $\beta_1$ ,  $\beta'_1$ ,  $\beta_2$  are the designations used for metal-rich phases in the respective phase diagrams [2]. Superscripts \* and \*\* denote Te and  $\text{Te}_2$ , respectively. KE = Knudsen effusion, Ms = mass spectrometry, MI = mass loss, T = torsion, Trans = transpiration.

tellurium is  $\text{Te}_2$  and (ii)  $\text{Te}_2(\text{g})$  can be treated as an ideal gas. The first conclusion has been confirmed by recent atomic absorption spectroscopic measurements [58] but the second one is in contradiction to the work of ref. [17] and particularly ref. [59] who treated the saturated vapor as non-ideal, showed the ratio  $p^\circ(\text{Te}_2)/p^\circ(\text{total})$  to be close to 1 up to about 1000 K and 0.934 at 1200 K and interpreted it as the fugacity coefficient of nonideal  $\text{Te}_2(\text{g})$ .

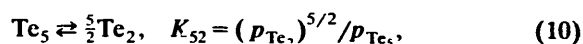
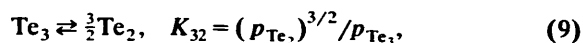
In the light of the foregoing discussion, the thermodynamic functions for  $\text{Te}(\text{c}, l)$ ,  $\text{Te}_2(\text{g})$  and  $\text{Te}(\text{g})$  given by Gronvold et al. [19] along with the new value of  $253300 \text{ J mol}^{-1}$  for the dissociation energy of  $\text{Te}_2(\text{g})$  [32] are selected for all subsequent calculations. This gives the equilibrium constant for the reaction



as

$$\log K_{21} = -6664/T + 2.09 - 3.8 \times 10^{-5}T - 2.302 \times 10^3/T^2 - 0.2525 \log T. \quad (8)$$

Making use of this equilibrium constant in conjunction with the equilibria (9) and (10),



the  $\log p$  versus  $1/T$  space of fig. 6 is delineated into the regions of predominance of vapor species containing more than 99%  $\text{Te}(\text{g})$  and 99%  $\text{Te}_2(\text{g})$ . The equilibrium constants,  $K_{32}$  and  $K_{52}$  were calculated at 800, 1000 and 1200 K from the mole ratios of the species given by Gronvold et al. [19].

### 2.3. Dissociation pressures of metal tellurides

The fundamental questions concerning the chemical state of Te in the fuel element are: what chemical compounds are formed by Te and where in the fuel element are they located? For this purpose, the partial pressures of tellurium over the tellurides of the relevant metals are the most important thermodynamic

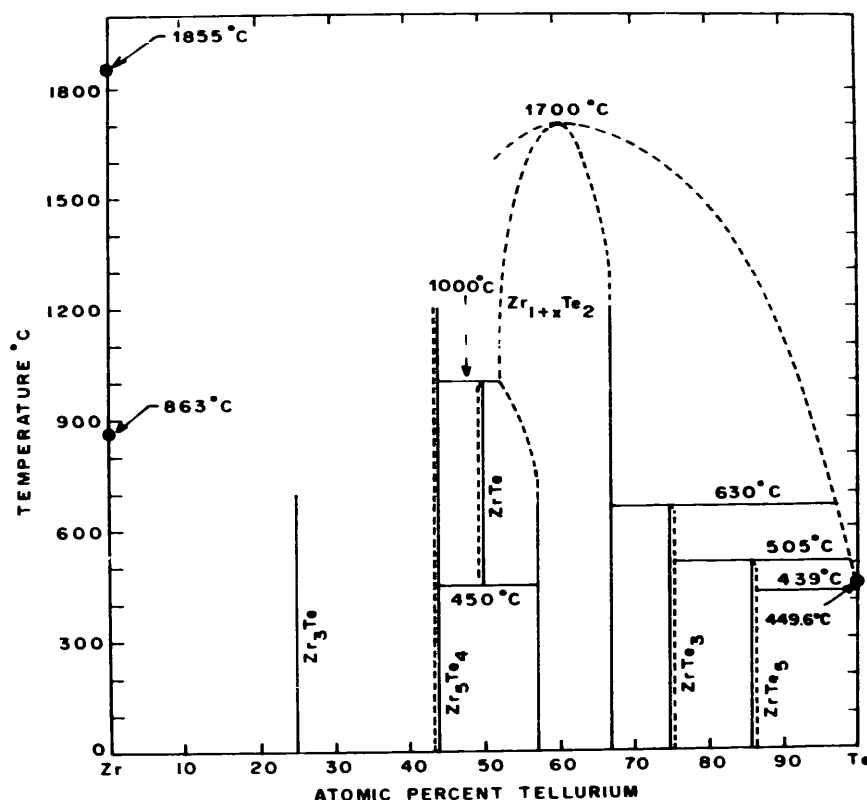


Fig. 7. Phase diagram of the system zirconium-tellurium.





space is delineated into domains of applicability of various techniques, e.g., the isopiestic, the Knudsen effusion and the emf. The domain of the static techniques including isopiestic is shown by horizontal hatches with 10 Pa as the lower pressure limit. The Knudsen effusion technique is bounded by the upper and lower pressure limits of 10 and  $10^{-7}$  Pa. This is shown by the left diagonal hatches. The oxide-based solid electrolyte galvanic cell has an upper temperature limit of 1000 K owing to the melting of  $\text{TeO}_2$  at 1006 K and a lower limit of 723 K below which the cell resistance is too high. This domain is indicated by right diagonal hatches. As seen in the figure, there are domains of overlap between the isopiestic and emf as well as Knudsen effusion and emf techniques. The dissociation pressure data selected from table 3 are also plotted in fig. 6.

In the cases of Ce, Sm and Ba the vaporization is congruent and the vapor pressure is made of equal contribution of  $\text{M(g)}$  and  $\text{Te(g)}$ . Although not plotted in fig. 6 the solid tellurides of alkaline and rare earths (Ba, Ce, Sm) are by far the most stable. The next in importance among the fission product tellurides shown

in fig. 6 are those of Ag, Mo and Pd. For another important f.p., namely, Zr, to the best of our knowledge, the dissociation pressures have not been measured. Recently Yamanaka et al. [79] have tried to estimate the dissociation pressure over  $\text{ZrTe}_2$  and  $\text{ZrTe}_3$  using the calorimetrically determined  $\Delta_f G^\circ$  value of  $\text{ZrTe}_2(\text{s})$  [80]. The phase diagram of the Zr-Te system [81] given in fig. 7 shows the peritectic decomposition of  $\text{ZrTe}_3$  into  $\text{ZrTe}_2$  and a tellurium-rich melt at 903 K. The concentration of Zr in this melt is about 2–5 at%. Thus at 900 K the partial pressure of  $\text{Te}_2$  over a  $\text{ZrTe}_2$ - $\text{ZrTe}_3$  mixture is close to that of  $\text{Te(l)}$ . Assuming  $\beta$ -Zr to be coexisting with  $\text{ZrTe}_2(\text{s})$  between 1300 and 1500 K the partial pressures of  $\text{Te}_2$  calculated from the  $\Delta_f G^\circ$  value of  $\text{ZrTe}_2(\text{s})$  are plotted in fig. 6 as a dotted line. This represents a tentative limit of stability of the Zr-rich phase and shows that the predominant species in the gas phase is  $\text{Te(g)}$ . The vaporization of  $\text{Cs}_2\text{Te(s)}$  in the temperature range of 850–1000 K was assumed to be congruent by Cordfunke et al. [82], while Portman et al. [83] found the vaporization of the melt at 1146 K to be incongruent. The partial pressure of  $\text{Te}_2(\text{g})$  over stoichiometric

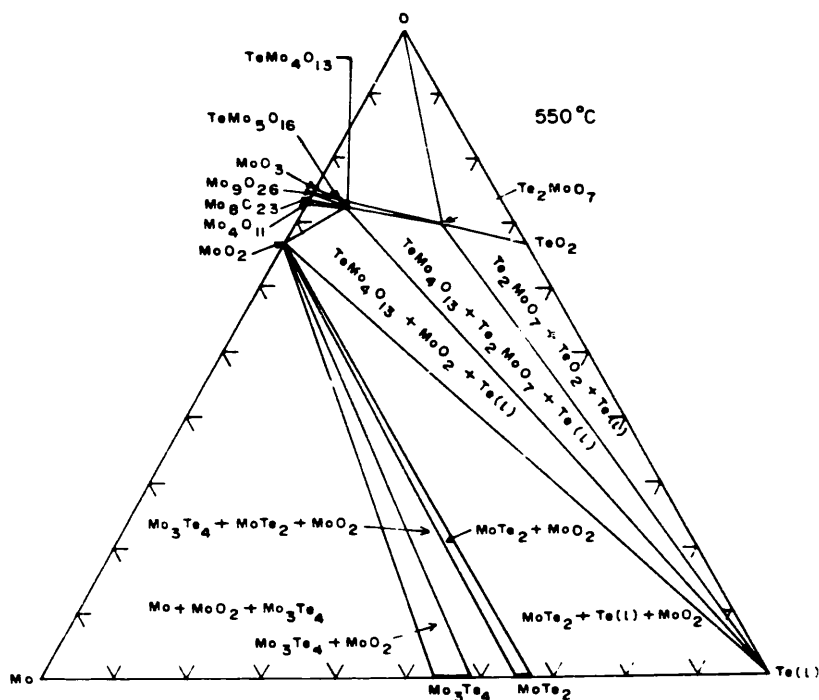


Fig. 9. Isothermal section of the phase diagram of the system Mo-Te-O at 550°C.

$\text{Cs}_2\text{Te}$ -melt between 1083 and 1146 K is plotted in fig. 6 and is given by the approximate relation (11)

$$\log p_{\text{Te}_2} = -7600/T + 6.059 \quad (p \text{ in Pa and } T \text{ in K}). \quad (11)$$

The free energy of formation of  $\text{Cs}_2\text{Te}$  (c, l) at the congruent melting point of 1083 K calculated from the above data, however, turns out to be 25 kJ less negative than the calorimetrically-determined free energy of formation of  $\text{Cs}_2\text{Te}$ (c) [84,85].

Thus it is clear that reliable data on the dissociation pressures over the metal-rich regions of the systems Zr-Te, Cs-Te and Pd-Te are lacking and as fig. 6 shows, Knudsen effusion seems to be the most appropriate technique available for these measurements.

#### 2.4. Ternary systems

Important ternary compounds of the M-Te-O systems are  $\text{UOTe}$  [86],  $\text{U}_2\text{O}_2\text{Te}$  [87],  $\text{Pu}_2\text{O}_2\text{Te}$  [88,89],  $\text{ThOTe}$  [90],  $\text{RE}_2\text{O}_2\text{Te}$  (RE = Ce, Nd, La) [91],  $\text{BaTeO}_3$  [92] and  $\text{Cs}_2\text{TeO}_3$  [93]. The phase diagram of the Zr-Te-O system presented in fig. 8 is the corrected version of the one given by Yamanaka et al. [94]. It

shows  $\text{ZrTe}_3\text{O}_8$  to be a relatively unstable compound. So are the ternary compounds in the Mo-Te-O [95] and Ag-Te-O [96] systems as seen in their respective phase diagrams given in figs. 9 and 10. The possibility of the formation of oxytellurides of the actinides and lanthanides is indicated from the ternary phase diagram of the prototypical U-Te-O system [97] presented in fig. 11. In the Cs-Te-O system, the ternary compounds  $\text{Cs}_2\text{TeO}_3$ ,  $\text{Cs}_2\text{Te}_2\text{O}_5$ ,  $\text{Cs}_2\text{Te}_4\text{O}_9$ , and  $\text{Cs}_2\text{Te}_4\text{O}_{12}$  have been identified [93,98]. The ternary phase diagram given in fig. 12 shows that the only solid compound of interest in this system is  $\text{Cs}_2\text{TeO}_3$ . All other compound phases melt below 850 K [98]. Very little information is available on the Ba-Te-O system which is depicted in fig. 13. Although the tie-lines are drawn assuming a similarity with the Zr-Te-O system,  $\text{BaTeO}_3$  seems to be a stable compound and might coexist with BaTe. A review of Ni-Te-O, Cr-Te-O, Fe-Te-O, Sn-Te-O, Pd-Te-O and Ru-Te-O systems [99] gave no indication of any ternary phase which could be of relevance.

Other ternary systems of interest would involve the clad components, such as the systems Fe-Cr-Te, Cr-Ni-Te, Fe-Ni-Te or would involve more than one

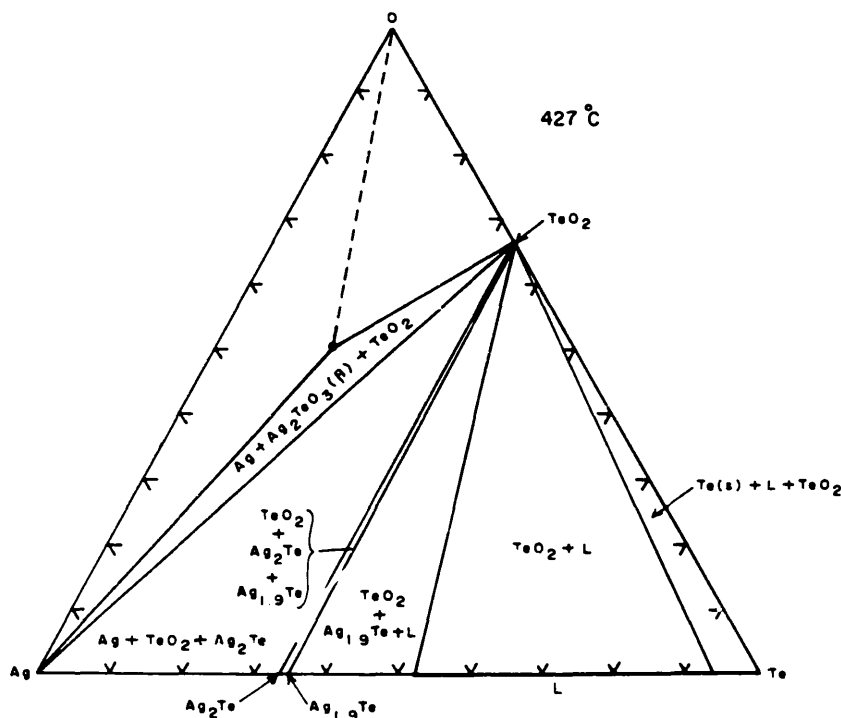


Fig. 10. Isothermal section of the phase diagram of the system Ag-Te-O at 427°C.

fission product, e.g. the system Pd–Rh–Te which is identified in the vitrified waste [100,101] or the system Pd–Ag–Te which is reported to form a very low melting eutectic [102]. No comprehensive study of ternary phase diagrams for the Fe–Cr–Te, Ni–Cr–Te, Fe–Ni–Te has yet been made. It is generally known that metal-rich tellurides of Ni or Cr form such ternary phases as  $\text{Fe}_{1.5}\text{Ni}_{1.5}\text{Te}_2$ ,  $(\text{Cr}_{1-x}\text{Fe}_x)_3\text{Te}_4$  or  $(\text{Cr}_{1-x}\text{Ni}_x)_3\text{Te}_4$  [103]. Only recently the  $\text{Cr}_3\text{Te}_4$ – $\text{FeTe}_2$  section of the Fe–Cr–Te system was investigated [104].

#### 2.4.1. The gaseous species containing tellurium

The metal tellurides having any significant stability in the gas phase are those of tin and caesium. Gaseous tellurides of tin are thermodynamically well characterized [105].  $(\text{CsTe})_2(\text{g})$  seems to be the most important gaseous species of the Cs–Te system [83], for which no thermodynamic data is available. Stabilities of gaseous species of  $\text{MTe}(\text{g})$  type for lanthanides (La, Ce, Nd, Pr, Sm) [106,107] and actinides (Th, U, Pu) [10] have been estimated. The ternary species  $\text{Cs}_2\text{TeO}_3(\text{g})$  has recently

been identified [83] but its thermodynamic stability is not known. The rest of the Te-bearing gaseous species which might be of significance are those combined with the nonmetals like O, H and I.

#### 2.5. Thermodynamic data

The thermodynamic data of the selected condensed phases and gaseous species are summarized in tables 4 and 5. The tables are structured in accordance with the current trend. The sources of data are given in appendix A.

### 3. Conclusion

Integration of phase diagram and thermodynamic data is the current paradigm in the field of chemical thermodynamics of materials. This was attempted in the present work for a few selected tellurium-bearing systems, the need for which was felt long ago [108] and

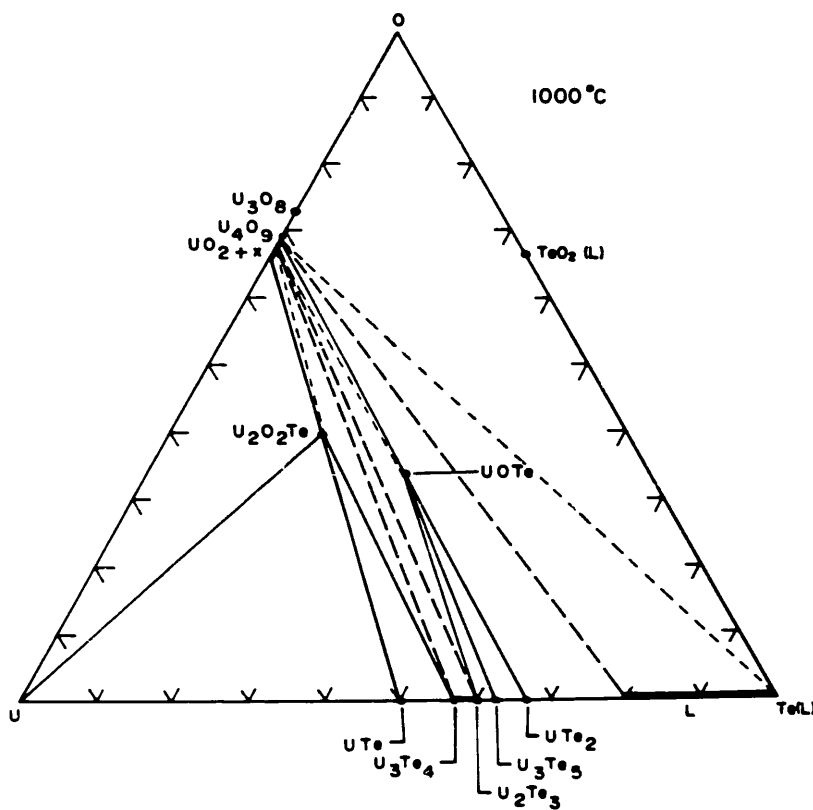


Fig. 11. Isothermal section of the phase diagram of the system U–Te–O at 1000°C.

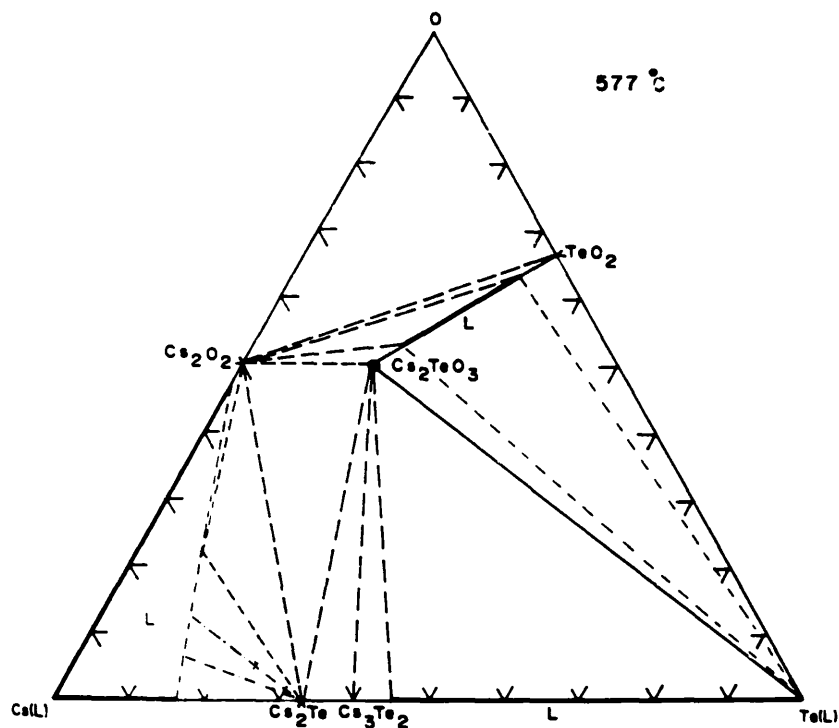


Fig. 12. Isothermal section of the phase diagram of the system Cs-Te-O at 577°C.

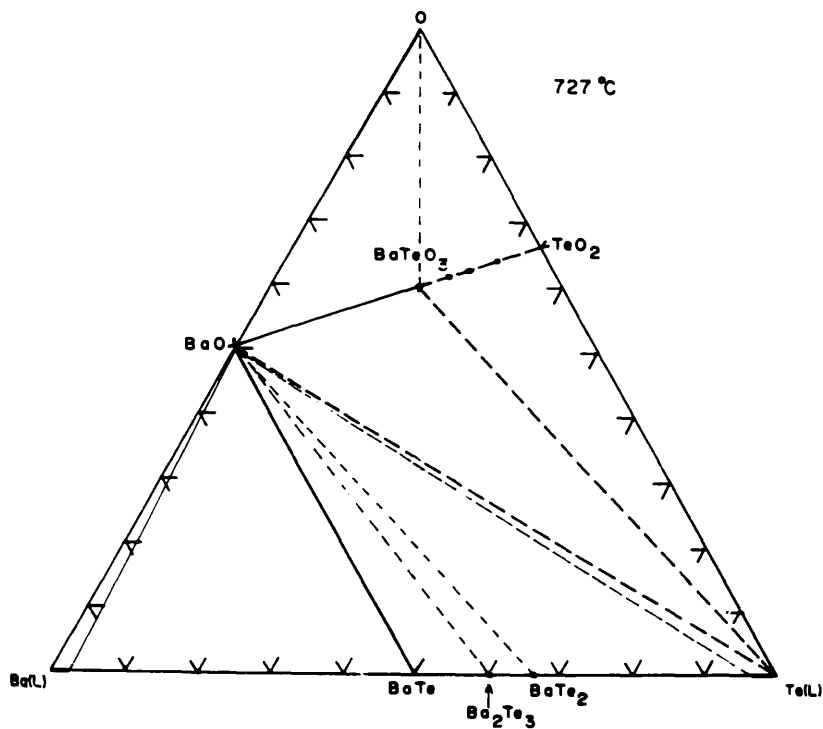


Fig. 13. Isothermal section of the phase diagram of the system Ba-Te-O at 727°C.

Table 4

Thermodynamic data of tellurium-bearing condensed phases. Parentheses indicate estimated data

Phase	$C_p = a + bT + cT^2 + dT^{-2}$ (J/mol K)					$\Delta_f H_{298}^\circ$ (J/mol)	$S_{298}^\circ$ (J/mol K)	$\Delta_{tr} H^\circ$ (J/mol)	$\Delta_{tr} S^\circ$ (J/mol K)
	Temperature (K)	$a$	$b \times 10^3$	$c \times 10^7$	$d \times 10^{-5}$				
Te(c)	298–722.6	33.6687	31.5674	314.425	–3.10029	0	49.22	17376	24.046
Te(l)	722–1020	–629.492	0.095046	–3868.12	989.315	–	–	–	–
Cs <sub>2</sub> Te	298–1000	90.52	–19.15	248.3	–7.729	–362100	185.1	–	–
Ag <sub>2</sub> Te	298–420	4.903	278.6	–1797	11.58	–32900	171.5	–	–
SnTe	298–1078	48.95	10.15	–0.3894	4.754	–59220	104.4	–	–
BaTe	298–1700	51.53	2.443	25.28	–0.1506	–453000	(97.9)	–	–
NdTe	298–2000	48.367	6.108	0	0	(–301200)	(97.5)	–	–
CeTe	298–1700	51.53	2.443	25.28	–0.1506	–286000	(97.9)	–	–
PrTe	298–2000	48.116	6.150	0	0	(–301200)	(97.5)	–	–
LaTe	298–2000	48.116	6.150	0	0	(–301200)	88.3	–	–
SmTe	298–1700	51.53	2.443	25.28	–0.1506	–390300	(97.9)	–	–
ThTe	298	–	–	–	–	(–243000)	(96)	–	–
UTe	298	–	–	–	–	–182420	(109)	–	–
PuTe	298	–	–	–	–	(–217500)	(109)	–	–
RuTe <sub>2</sub>	298–1500	86.48	–22.79	174.6	–6.3555	–141700	(95.0)	–	–
ZrTe <sub>2</sub>	298–1500	73.48	9.052	22.33	–2.015	–294100	124.24	–	–
Fe <sub>0.53</sub> Te <sub>0.47</sub>	298–900	35.31	–23.33	259.9	–4.098	–12347	42.17	–	–
Mo <sub>0.43</sub> Te <sub>0.57</sub>	298–1600	26.63	0.7817	0.2274	–1.081	–33046	37.14	–	–
Cr <sub>0.43</sub> Te <sub>0.57</sub>	298–900	41.75	–55.94	550.0	–1.824	–34338	41.87	–	–
Ni <sub>0.60</sub> Te <sub>0.40</sub>	298–490	–6.064	98.48	–681.5	–7.700	–26040	(40)	384	0.78
	490–609	1439.0	–3717	27590	–598.2	–	–	664	1.16
	609–1060	306.0	–548.3	3095	–204.7	–	–	–	–
Cs <sub>2</sub> TeO <sub>3</sub>	298–1084	109.9	80.28	–0.2916	1.874	–993800	(232)	–	–

Table 5

Thermodynamic data of tellurium-bearing gaseous species

Species	$C_p = a + bT + cT^2 + dT^{-2}$ (J/mol K)					$\Delta_f H_{298}^\circ$ (J/mol)	$S_{298}^\circ$ (J/mol K)
	Temperature (K)	$a$	$b \times 10^3$	$c \times 10^7$	$d \times 10^{-5}$		
Te	298–3000	18.73	2.588	–1.543	1.349	209450	182.603
Te <sub>2</sub>	298–3000	41.49	2.940	–7.059	–5.955	163176	258.822
TeO	298–3000	42.54	–0.3994	9.043	–3.022	92000	235.425
TeO <sub>2</sub>	298–3000	55.84	0.6297	3.271	–9.941	–54800	272.795
TeO(OH) <sub>2</sub>	298–3000	95.68	22.31	38.33	–15.90	–430000	332.477
H <sub>2</sub> Te	298–3000	34.54	17.44	–34.38	3.763	99700	228.358
TeI	298–3000	37.40	0.3797	–0.03094	–0.6298	–	266.777
TeI <sub>2</sub>	298–3000	58.17	0.02785	–0.06083	–1.221	–	345.564
TeI <sub>4</sub>	298–3000	108.1	0.02205	–0.04865	–1.845	5700	456.211
TeOI <sub>2</sub>	298–3000	81.07	1.755	–3.768	–6.070	–40000	373.140
SnTe	298–3000	37.82	–0.3925	–2.249	–1.014	161000	264.037
Sn <sub>2</sub> Te <sub>2</sub>	298–3000	83.11	0.02857	–0.06256	–1.814	568000	399.839
SnTe <sub>2</sub>	298–3000	62.32	0.03569	–0.07759	–1.501	401000	320.170

was being felt increasingly in recent years for such applications as, in the thermodynamic modeling of clad-f.p. interactions [109] or the chemical constitution of the fuel-clad gap [110], of the chemical state of the irradiated oxide fuel [111,112] or of the release behavior under accident conditions [113].

In this work, the systems which are of relevance are enumerated, the data of recent origin are evaluated and a database of selected systems are presented. This is in continuity with the comprehensive work of Mills [18] on thermodynamic data for some metal-tellurium systems (1974), with that of Blackburn and Johnson (1982) [114] who tabulated the free energy data of the relevant metal tellurides, with the work of Gronvold, Drowart and Westrum (1984) [10], our own work on the binary phase diagrams of M-Te systems (1984–1989) [1,2] and with the most recent and exhaustive compilation of Cordfunke and Konings (1990) [115] which gave the thermodynamic data for most of the gaseous species and a few of the condensed phases.

## Acknowledgement

The authors thank Dr. H. Kleykamp for his valuable comments on the work.

## Appendix A. Notes on phase diagrams and thermodynamic data

### A1. Phase diagram

**Pd-Te:** The diagram given in fig. 1 is the result of evaluation of the work of ref. [3] and of refs. [116–118]. In this evaluation the solid solubility of tellurium in palladium below 600°C is assigned a larger value than in a recent assessment [119].

**Rh-Te:** The diagram given in fig. 2 is the result of combining the work of refs. [4] and [120]. The original construction [4] shows an unusual asymmetry in the tellurium-rich side whereas the alternative construction proposed by Okamoto [121] does not conform to the experimental data [120]. Hence, a miscibility gap in the tellurium-rich liquid and a monotectic temperature close to 1075°C are speculated.

**U-Te and U-Te-O:** The phase diagram of the U-Te system presented in ref. [10] is in good agreement with a recent work on the tellurium-rich phases of uranium [122] and hence, is accepted. The three-phase regions of the U-Te-O system in fig. 11 are

drawn in accordance with ref. [97]. The tie-lines joining the various compositions of the  $\text{UO}_{2+x}$  phase are tentative.

**Cs-Te-O:** The diagram is drawn on the basis of the binary systems Cs-O, Te-O and Cs-Te. It was assumed that the Cs-O and Cs-Te melts are completely miscible giving rise to a Cs-Te-O melt which coexists with  $\text{Cs}_2\text{O}_2(\text{s})$  and  $\text{Cs}_2\text{Te}(\text{s})$ . The phase diagram of the Cs-O system given in ref. [115] has been used. The liquid phase on the pseudo-binary line,  $\text{Cs}_2\text{O}-\text{TeO}_2$ , is taken from the  $\text{TeO}_2-\text{Cs}_2\text{TeO}_3$  phase diagram given in ref. [115].

**Zr-Te-O:** The phase diagram of the pseudo-binary  $\text{ZrO}_2-\text{TeO}_2$  system has not been determined. The present diagram is based on the experimental work of ref. [94] in combination with the phase relations known in the binary Zr-Te system [2].

**Ba-Te-O:** The diagram is tentatively constructed on the basis of the binary Ba-Te system [8]. No definitive diagram for the pseudo-binary  $\text{BaO}-\text{TeO}_2$  system is available.

### A2. Thermodynamic data

**Iron telluride ( $\beta$ -phase:  $\text{Fe}_{1.1}\text{Te}$ ):** The composition of the iron-rich phase boundary of the  $\beta$ -phase is temperature-independent [123,124] but the actual composition is uncertain. According to the present evaluator this value is 46.0 at% Te. The thermodynamic data selected in table 4 is given for the composition 47.3 at% Te, for which  $S_{298}^\circ$  was derived from the low temperature heat capacity data [125]. The heat capacity equation is based on the data at high temperatures [126] and the standard heat of formation is taken from solution calorimetry [127]. The latter agrees well with the third-law value derived from vapor pressure measurements [60,61].

**Molybdenum telluride ( $\text{Mo}_3\text{Te}_4$ ):**  $S_{298}^\circ$  was derived from the low temperature heat capacity data [128], the heat capacity equation is based on estimated data [129] and the standard heat of formation is the third-law value derived from vapor pressure [66] and emf [130] data.

**Nickel telluride ( $\beta_2$ -phase:  $\text{Ni}_3\text{Te}_2$ ):** The composition of the nickel-rich phase boundary of the  $\beta_2$ -phase is 38.8 at% Te [2,131,132]. The thermodynamic data selected in table 4 is given for the composition 40.0 at% Te.  $S_{298}^\circ$  is estimated [18]. The heat capacity equation and heats of transition are based on experimental data [133]. The standard heat of formation is from solution calorimetry [127].

**Chromium telluride ( $\text{Cr}_3\text{Te}_4$ ):** Below 850 K the

chromium-rich phase boundary is 56.5 at% Te and is temperature-independent [134,135]. Above 850 K, the phase boundary varies with temperature. The thermodynamic data selected in table 4 is given for the composition 57 at% Te.  $S_{298}^{\circ}$  is calculated from the low temperature heat capacity data [136]. The heat capacity equation is based on experimental data [137,138]. The standard heat of formation is from high temperature gold solution calorimetry [138].

**Silver telluride** ( $\text{Ag}_2\text{Te}$ ):  $S_{298}^{\circ}$  was selected from ref. [18]. The low temperature heat capacity data yielded a slightly larger value [139]. The standard heat of formation is from high temperature reaction calorimetry [140].

**Ruthenium telluride** ( $\text{RuTe}_2$ ):  $S_{298}^{\circ}$  is estimated [115]. The heat capacity equation is based on experimental data [31]. The standard heat of formation is the third-law value obtained from vapor pressure data [31].

**Zirconium telluride** ( $\text{ZrTe}_2$ ): The metal-rich telluride is either  $\text{Zr}_3\text{Te}$  or  $\text{Zr}_5\text{Te}_4$  [2]. The thermodynamic data in table 4 is for the composition  $\text{ZrTe}_2$ .  $S_{298}^{\circ}$  is derived from the low temperature heat capacity data [80]. The heat capacity equation is based on experimental data obtained from drop calorimetry and the standard heat of formation from fluorine bomb calorimetry [80].

**Cesium telluride** ( $\text{Cs}_2\text{Te}$ ):  $S_{298}^{\circ}$  is derived from the low temperature heat capacity data [84]. The heat capacity equation is based on high temperature enthalpy increments [84] and the standard heat of formation from solution calorimetry [85].

**Tin telluride** ( $\text{SnTe}$ ):  $S_{298}^{\circ}$  is selected from the equilibrium data [115] because the low temperature heat capacity data [141,142] are in disagreement. The heat capacity equation is based on high temperature enthalpy increments by drop calorimetry [143] in preference to another similar measurement [144]. The standard heat of formation is from solution calorimetry [145].

**Barium telluride** ( $\text{BaTe}$ ):  $S_{298}^{\circ}$  is estimated [69]. The heat capacity equation is based on the data for  $\text{EuTe(s)}$  [146]. The standard heat of formation is obtained by combining the second-law value from the vapor pressure data for molten  $\text{BaTe}$  [69] with the heat of fusion of  $\text{BaTe}$  at 298 K. The latter is estimated by assuming the entropy of fusion of  $\text{BaTe(s)}$  as  $25 \text{ J K}^{-1} \text{ mol}^{-1}$  which gave the value of heat of fusion as  $43 \text{ kJ mol}^{-1}$  at the melting point (1730 K). This is further assumed to be independent of temperature.

**Cerium and samarium telluride** ( $\text{CeTe}$ ,  $\text{SmTe}$ ):  $S_{298}^{\circ}$  is estimated [18]. The heat capacity equation is based on the data for  $\text{EuTe(s)}$  [146]. The standard heat of

formation is from the second-law treatment of the vapor pressure data for  $\text{CeTe(s)}$  [71] and  $\text{SmTe(s)}$  [70].

**Neodymium and praseodymium telluride** ( $\text{NdTe}$ ,  $\text{PrTe}$ ):  $S_{298}^{\circ}$ , the heat capacity equations as well as the standard heats of formation are estimated [18].

**Lanthanum telluride** ( $\text{LaTe}$ ):  $S_{298}^{\circ}$  is obtained from the low temperature heat capacity data [147]. The heat capacity equation and the standard heat of formation are estimated [18].

**Thorium telluride** ( $\text{ThTe}$ ):  $S_{298}^{\circ}$  [18,148] and the standard heat of formation [18] are estimated.

**Plutonium telluride** ( $\text{PuTe}$ ):  $S_{298}^{\circ}$  and the standard heat of formation are estimated [10].

**Gaseous species:** The thermodynamic data for the gaseous species given in table 5 is taken from ref. [115].

## References

- [1] H. Kleykamp and G. Chattopadhyay, unpublished work.
- [2] G. Chattopadhyay and S.R. Bharadwaj, Evaluated Phase Diagrams of Binary Metal-Tellurium Systems of the D-Block Transition Elements, BARC-Report No. 1449 (1989).
- [3] M. Kelm, A. Goertzen, H. Kleykamp and H. Pentlinghaus, J. Less-Comm. Metals 166 (1990) 125.
- [4] Zh. Ding, H. Kleykamp and F. Thümmeler, J. Nucl. Mater. 171 (1990) 134.
- [5] T. Matkovic, M. Kesic-Recan and P. Matkovic, J. Less-Comm. Metals 138 (1988) L-1.
- [6] J. Rakotomavo, M.C. Baron and C. Petot, Metall. Trans. 12B (1981) 461.
- [7] K.A. Zinchenko, N.P. Luzhnaya, E.I. Yarembash and A.A. Eliseev, Inorg. Mater. 2 (1966) 1506.
- [8] Y.B. Lyskova and A.V. Vakhoboy, Inorg. Mater. 11 (1975) 1784.
- [9] E.I. Yarembash and E.S. Viglieva, Izvest. Akad. Nauk SSSR, Neorg. Mater. 6 (1970) 1572.
- [10] F. Gronvold, J. Drowart and E.F. Westrum, Jr., Chemical Thermodynamics of Actinide Elements and Compounds, part 4, Actinide Chalcogenides (IAEA, Vienna, 1984).
- [11] F.A. Shunk, Constitution of Binary Alloys, 2nd suppl. (McGraw-Hill, New York, 1969).
- [12] (a) K.A. Chuntunov, A.N. Orlov, S.P. Yatsenko, Yu.N. Grin' and L.D. Miroshnikova, Inorg. Mater. 18 (1982) 941.  
(b) K.A. Chuntunov, A.N. Kuzneal'tsov, V.M. Feldorov and S.P. Yatsenko, Inorg. Mater. 18 (1982) 93.
- [13] M.G. Adamson and J.E. Leighty, J. Nucl. Mater. 114 (1983) 327.
- [14] A. Bergmann, Z. Anorg. Allgem. Chem. 231 (1937) 269.
- [15] G. Prins and E.H.P. Cordfunke, J. Less-Comm. Metals 104 (1984) L1.



- [16] (a) P. Boettcher, *J. Less-Comm. Metals* 70 (1980) 263;  
(b) Z. Anorg. Allgem. Chem. 523 (1985) 145.
- [17] R. Hultgren, P.D. Desai, D.T. Hawkins, M. Glieser, K.K. Kelley and D.T. Wagman, *Selected Values of Thermodynamic Properties of Metals and Alloys* (American Society for Metals, Metals Park, Ohio, 1973).
- [18] K.C. Mills, *Thermodynamic Data for Inorganic Sulphides, Selenides and Tellurides* (Butterworths, London, 1974).
- [19] Ref. [10] pp. 153–160.
- [20] R.F. Brebrick, *High Temp. Sci.* 25 (1988) 187.
- [21] O. Kubaschewski and F.E. Wittig, *Z. Elektrochem.* 47 (1941) 433.
- [22] F. Gronvold and E.F. Westrum, Jr., unpublished work cited in ref. [115].
- [23] C.T. Anderson, *J. Am. Chem. Soc.* 59 (1937) 1036.
- [24] C.M. Slansky and L.V. Coulter, *J. Am. Chem. Soc.* 61 (1939) 564.
- [25] A.J. Leadbetter and A.P. Jeaps, *J. Phys. C6* (1973) 1546.
- [26] R.A. Medzhidov and S.M. Rasulov, *Inorg. Mater.* 11 (1975) 555.
- [27] S. Takeda, H. Okazaki and S. Tamaki, *J. Phys. Soc. Japan* 54 (1985) 1890.
- [28] C.E. Moore, *Atomic Energy Levels*, Notre Dame University, Radiation Laboratory, US Government Printing Office, Washington, DC, Rep. NSRDS-NBS-35, vols. 1–3 (1971).
- [29] J.E. Ruedy, *Phys. Rev.* 41 (1932) 588.
- [30] D.R. Stull and G.C. Sinke, *Thermodynamic Properties of the Elements, Advances in Chemistry Ser.* 18 (American Chemical Society Washington, DC, 1956).
- [31] S.R. Svendsen, *J. Chem. Thermodyn.* 9 (1977) 789.
- [32] J. Verges, C. Effantin, O. Babaky, J. d'Incan, S.J. Prosser and R.F. Barrow, *Phys. Scripta* 25 (1982) 338.
- [33] T.J. Stone and R.F. Barrow, *Can. J. Phys.* 53 (1975) 1976.
- [34] C. Effantin, J. d'Incan, J. Verges, M.T. Macpherson and R.F. Barrow, *Chem. Phys. Lett.* 70 (1980) 560.
- [35] R. Winter, I. Barnes, E.H. Fink, J. Wildt and F. Zabel, *Chem. Phys. Lett.* 86 (1982) 118.
- [36] F. Ahmed and E.R. Nixon, *J. Mol. Spectrosc.* 87 (1981) 101.
- [37] V.E. Bondybey and J.M. English, *Chem. Phys. Lett.* 72 (1980) 6479.
- [38] R.F. Barrow and R.P. Du Parc, *Proc. R. Soc. London A327* (1972) 279.
- [39] K.P. Huber and G. Herzberg, *Constants of Diatomic Molecules* (Van Nostrand Reinhold, New York, 1979).
- [40] W.M. Dukelskii and N.I. Ionov, *Dokl. Akad. Nauk SSSR* 81 (1951) 767.
- [41] G.P. Ustygov and E.N. Vigdorovich, *Izvest. Akad. Nauk SSSR Neorg. Mater.* 4 (1968) 2022.
- [42] V.S. Ban and B.E. Knox, *J. Chem. Phys.* 51 (1969) 524.
- [43] D. Bayer, *ACM Student Report* (1965), cited in ref. [18].
- [44] Yu. M. Ivanov, *Russ. J. Phys. Chem.* 47 (1973) 909.
- [45] A. Neubert, *High Temp. Sci.* 10 (1978) 261.
- [46] K.H. Grupe, K. Hellwig, L. Kolditz, *Z. Phys. Chem. (Leipzig)* 255 (1974) 1015.
- [47] A. Horeau, B. Caband and R. Uzan, *J. Phys. (Paris)* 39 (1978) L305.
- [48] M. Jenunthome, Ph.D. Thesis, University of Brussels (1962), cited in ref. [19].
- [49] R. Viswanathan, M. Sai Baba, D. Darwin Albert Raj, R. Balasubramanian and C.K. Mathews, in *Advances in Mass Spectrometry*, ed. J.F.J. Todd (Wiley, New York, 1986) p. 1087.
- [50] L.S. Brooks, *J. Am. Chem. Soc.* 74 (1952) 227.
- [51] E.H. Baker, *J. Chem. Soc. A* (1967) 1558.
- [52] A.A. Kudryatsev and G.P. Ustygov, *Russ. J. Inorg. Chem.* 6 (1961) 1227.
- [53] R.E. Machol and E.F. Westrum, Jr., *J. Am. Chem. Soc.* 80 (1958) 2950.
- [54] K. Niwa and Z. Sibata, *J. Chem. Soc. Japan* 61 (1940) 667.
- [55] I.V. Korneeva, A.S. Pashinkin, A.V. Novoselova and Yu. A. Priselov, *Russ. J. Inorg. Chem.* 2 (1957) 1720.
- [56] R.F. Brebrick, *J. Phys. Chem.* 72 (1968) 1032.
- [57] L. Malaspina, R. Gigli and G. Bardi, *Rev. Int. Hautes Temp. et Réfract.* 9 (1972) 131.
- [58] S. Helle, B. Yazar and T. Wildeman, *Ind.-Univ. Adv. Mater. Conf., TMS Annual Meeting* (1987) p. 95, cited in ref. [115].
- [59] Yi-Gao Sha, Kuo Tong Chen, R. Fang and R. Brebrick, *J. High-Temp. Sci.* 25 (1988) 153.
- [60] R. Prasad, S. Mohapatra, V.S. Iyer, Z. Singh, V. Venugopal and D.D. Sood, *J. Chem. Thermodyn.* 20 (1988) 453.
- [61] (a) B. Saha, R. Viswanathan, M. Sai Baba, D. Darwin Albert Raj, R. Balasubramanian, D. Karunasagar and C.K. Mathews, *J. Nucl. Mater.* 130 (1985) 316.  
(b) B. Saha, R. Viswanathan, M. Sai Baba and C.K. Mathews, *High Temp. High Press.* 20 (1988) 47.
- [62] R. Prasad, V.S. Iyer, Z. Singh, V. Venugopal, S. Mohapatra and D.D. Sood, *J. Chem. Thermodyn.* 20 (1988) 319.
- [63] R. Viswanathan, M. Sai Baba, D. Darwin Albert Raj, R. Balasubramanian, B. Saha and C.K. Mathews, *J. Nucl. Mater.* 167 (1989) 94.
- [64] R. Prasad, V.S. Iyer, V. Venugopal, V. Sundaresh, Z. Singh and D.D. Sood, *J. Chem. Thermodyn.* 19 (1987) 891.
- [65] R. Viswanathan, M. Sai Baba, D. Darwin Albert Raj, R. Balasubramanian, B. Saha and C.K. Mathews, *J. Nucl. Mater.* 149 (1987) 302.
- [66] R. Viswanathan, R. Balasubramanian and C.K. Mathews, *J. Chem. Thermodyn.* 21 (1989) 1183.
- [67] G. Krabbes, *Z. Anorg. Allgem. Chem.* 543 (1986) 97.
- [68] V.K. Slovyanskikh, G.V. Ellert and E.I. Yarembash, *Izv. Akad. Nauk SSSR Neorg. Mater.* 3 (1967) 1133.
- [69] J. Ludwigs and T. Petzel, *Rev. de Chim. Miner.* 123 (1986) 253.
- [70] T. Petzel and J. Ludwigs, *High-Temp. Sci.* 24 (1987) 79.

- [71] T. Koyama and M. Yamawaki, *J. Nucl. Mater.* 152 (1988) 30.
- [72] G.M. Zhiteneva, Y.M. Rumnyatsev and F.M. Bolandz, *Trudy. Vost. Sib. Akad. Nauk SSSR* 41 (1962) 151.
- [73] K.C. Mills, *J. Chem. Thermodyn.* 4 (1972) 903.
- [74] M. Adami, D. Ferro, V. Piacente and P. Scardala, *High-Temp. Sci.* 123 (1987) 173.
- [75] Y.A. Dutchak, I.A. Tishchenko and N.M. Korenchuk, *Izv. Akad. Nauk SSSR Neorg. Mater.* 13 (1977) 1980.
- [76] H. Ipser, *Z. Metallk.* 73 (1982) 151.
- [77] C. Mallika and O.M. Sreedharan, *J. Nucl. Mater.* 167 (1989) 181.
- [78] K. Hsieh, M. Sieng Wei and Y.A. Chang, *Z. Metallk.* 74 (1989) 330.
- [79] S. Yamanaka, M. Katsura and M. Miyake, *Technol. Rep. Osaka Univ.* 38 (1988) 59.
- [80] G.K. Johnson, W.T. Murray, E.H. Van Deventer and H.E. Flotow, *J. Chem. Thermodyn.* 17 (1985) 751.
- [81] H. Sodeck, H. Mikler and K.L. Komarek, *Monatsh. Chem.* 110 (1979) 1.
- [82] E.H.P. Cordfunke, F. Kleverlaan and W. Ouweltjes, *Thermochim. Acta* 102 (1986) 387.
- [83] R. Portman, M.J. Quinn, N.H. Sagert, P.P.S. Saluja and D.J. Wren, *Thermochim. Acta* 144 (1989) 21.
- [84] E.H.P. Cordfunke and W. Ouweltjes, *J. Chem. Thermodyn.* 19 (1987) 293.
- [85] E.H.P. Cordfunke and W. Ouweltjes, J.C. Van Miltenberg and A. Schuijf, *J. Chem. Thermodyn.* 19 (1987) 377.
- [86] A.J. Klein-Haneveld and F. Jellinek, *J. Inorg. Nucl. Chem.* 26 (1964) 1127.
- [87] E.W. Breeze and N.H. Brett, *J. Nucl. Mater.* 40 (1971) 113.
- [88] M. Allbutt and A.R. Junkinson, *AERE Report R-5541* (1967).
- [89] J.M. Constantani, D. Damien, C.H. de Novion, A. Blaise, A. Cusson, H. Abazli and M. Pages, *J. Solid State Chem.* 47 (1983) 219.
- [90] R.W.M. D'Eye and R.G. Sellman, *J. Chem. Soc.* 3760 (1954).
- [91] Y. Abbas, Thesis, University of Grenoble (1976), cited in T. Thevenin, J. Jove and M. Pages, *Mater. Res. Bull.* 20 (1985) 1075.
- [92] J. Wroblwska, A. Erb, J. Dobrowolski and W. Freundlich, *Rev. Chim. Mineral.* 16 (1979) 112.
- [93] B.O. Loopstra and K. Goubitz, *Acta Crystallogr.* C42 (1986) 520.
- [94] S. Yamanaka, N. Takatsuka, M. Katsura and M. Miyaka, *J. Nucl. Mater.* 161 (1989) 210.
- [95] J.C.J. Bart, G. Petini and N. Girodano, *Z. Anorg. Allgem. Chem.* 413 (1975) 180.
- [96] S.R. Bharadwaj and G. Chattopadhyay, *J. Solid State Chem.* 80 (1989) 256.
- [97] E.W. Breeze, N.H. Brett and J. White, *J. Nucl. Mater.* 39 (1971) 157.
- [98] E.H.P. Cordfunke and V.M. Smit Goren, *Thermochim. Acta* 80 (1984) 181.
- [99] G. Chattopadhyay, unpublished work.
- [100] H. Kleykamp, *Nucl. Technol.* 80 (1988) 412.
- [101] C. Krause and B. Luckscheiter, *J. Mater. Res.* 6 (1991) 2535.
- [102] I.I. Chernyanev, N.N. Zheligovskaya, M.K. Borisenkova and N.A. Subbotina, *Russ. J. Inorg. Chem.* 13 (1968) 848.
- [103] A.L.N. Stevels, *Philips Res. Rep. Suppl.* 9 (1969) 27.
- [104] K.V. Eremin, T.I. Koneshova and V.M. Novotorotsev, *Zh. Neorg. Khim.* 35 (1990) 2629.
- [105] J. Hoeft and E. Tiemann, *Z. Naturforsch.* 23A (1968) 1034.
- [106] C. Bergman, P. Coppens, J. Drcwart and S. Smoes, *Trans. Faraday Soc.* 66 (1970) 845.
- [107] B. Eichler, H. Rossbach and H. Gäggeler, *J. Less-Comm. Metals* 163 (1990) 297.
- [108] M.G. Adamson, G. Schumacher, J.D. Navratil and H. Sundermann, *At. Energy Rev.* 18 (1980) 247.
- [109] O. Götzmann, *J. Nucl. Mater.* 84 (1979) 39.
- [110] M.G. Adamson, E.A. Aitken and B. Lindemer, *J. Nucl. Mater.* 130 (1985) 375.
- [111] H. Kleykamp, *J. Nucl. Mater.* 131 (1985) 221.
- [112] E.H.P. Cordfunke and R.J.M. Konings, *J. Nucl. Mater.* 130 (1985) 82; 152 (1988) 301.
- [113] D. Cubicciotti and B.R. Sehegal, *Nucl. Technol.* 65 (1984) 266.
- [114] P.E. Blackburn and C.E. Johnson, *ANL* 82-42 (1982).
- [115] *Thermochemical Data for Reactor Materials and Fission Products*, ed. E.H.P. Cordfunke and R.J.M. Konings (North-Holland, Amsterdam, 1990).
- [116] G. Chattopadhyay, Y.J. Bhatt and S.K. Khera, *J. Less-Comm. Metals* 123 (1986) 251.
- [117] H. Ipser and W. Schuster, *J. Less-Comm. Metals* 125 (1986) 183.
- [118] W.S. Kim and G.Y. Chao, *J. Less-Comm. Metals* 162 (1990) 61.
- [119] H. Okamoto, *J. Phase Equilibria* 13 (1992) 73.
- [120] A. Kjekshus, T. Rakke and A.F. Andressen, *Acta Chem. Scand.* A32 (1978) 209.
- [121] H. Okamoto, *J. Phase Equilibria* 12 (1991) 121.
- [122] D.R. Boeheme, M.C. Nichols, R. Snyder and D.P. Mathais, *J. Alloys and Compounds* 179 (1992) 37.
- [123] H. Ipser, K.L. Komarek and H. Mikler, *Monatsh. Chem.* 105 (1974) 1322.
- [124] H. Okamoto and L.E. Tanner, *Bull. Alloy Phase Diagr.* 11 (1990) 371.
- [125] F. Gronvold, H. Haraldsen and J. Vihovde, *Acta Chem. Scand.* 8 (1954) 1927.
- [126] J. Mikler, H. Ipser and K.L. Komarek, *Monatsh. Chem.* 105 (1974) 977.
- [127] N.K. Shukla, R. Prasad, K.N. Roy and D.D. Sood, *J. Chem. Thermodyn.* 22 (1990) 899.
- [128] E.B. Amitin, Yu.F. Meninkov, O.A. Nabutovskaya, V.N. Naumov, I.E. Paukov and G. Krabbes, *Zhur. Fiz. Khim.* 64 (1990) 1755.
- [129] L. Brewer, R.H. Lamoreaux, R. Ferro, R. Marazza and K. Girgis, in *Molybdenum: Physico-Chemical Properties*

- of its Compounds and Alloys, At. Energy Rev. Special Issue No. 7, (IAEA, Vienna, 1980).
- [130] C. Mallika and O.M. Sreedharan, J. Nucl. Mater. 170 (1990) 934.
- [131] K.O. Klepp and K.L. Komarek, Monatsh. Chem. 103 (1972) 934.
- [132] S.Y. Lee and P. Nash, in Phase Diagrams of Binary Nickel Alloys, ed. P. Nash (ASM, Metals Park, OH, 1991) p. 330.
- [133] F. Gronvold, N.J. Kvseth and A. Sveen, J. Chem. Thermodyn. 4 (1972) 337.
- [134] H. Ipser, K.O. Klepp and K.L. Komarek, J. Less-Comm. Metals 92 (1983) 265.
- [135] G. Chattopadhyay, J. Phase Equilibria, submitted.
- [136] F. Gronvold and E.F. Westrum, Jr., Z. Anorg. Allgem. Chem. 328 (1964) 272.
- [137] F. Gronvold, J. Chem. Thermodyn. 5 (1973) 545.
- [138] P. Gunia, Thesis, Gesamthochschule Siegen, 1979.
- [139] P.V. Gulyaev and A. Petrov, Sov. Phys. Solid State 1 (1959) 330.
- [140] R. Castanet and C. Bergman, J. Chem. Thermodyn. 11 (1979) 83.
- [141] A.J. Bevelo, H.R. Shanks and D.E. Eckels, Phys. Rev. 13 (1976) 3523.
- [142] M. Wohlrab, Ann. Physik (N.F.) 17 (1966) 89.
- [143] R. Blachnik, R. Igel and P. Wahlbrecht, Z. Naturforsch. 29A (1974) 1198.
- [144] R.A. Medzhidov and S.M. Rasulov, Russ. J. Phys. Chem. 53 (1979) 100.
- [145] R. Castanet, Y. Claire and M. Laffitte, High Temp.-High Press. 4 (1972) 343.
- [146] O.D. McMasters, K.A. Gschneidner, E. Kaldis and G. Sampitro, J. Chem. Thermodyn. 6 (1974) 845.
- [147] V.V. Tikhonov, A.V. Golubkov and I.A. Smirnov, Fiz. Tverd. Tela. 8 (1966) 3578.
- [148] E.F. Westrum, Jr. and F. Gronvold, Proc. Symp. on Thermodynamics of Nuclear Materials (IAEA, Vienna, 1962) p. 3.
- [149] Y. Baskin and S.D. Smith, J. Nucl. Mater. 37 (1970) 209.